Published Online First: March, 2024
https://doi.org/10.21123/bsj.2024.8319
P-ISSN: 2078-8665 - E-ISSN: 2411-7986
Baghdad Science Journal

Synthesis, characterization, industrial and biological studies of azo dye ligand and their some metallic ions

***Abaas Obaid Hussein* [*1], *Rana Abdulilah Abbas* [2], *Jinan M. M. Al-Zinkee* [3], *AmerJ.Jarad** [*4]**

[1]Medical Laboratory Technology Department, College of Medical Technology, the Islamic University, Najaf, Iraq.
[2]Chemical Industrial Department, Institute of Technology, Middle Technical University, Baghdad, Iraq.
[3]Department of Chemistry, College of science, University of Diyala, Diyala, Iraq.
[4]Department of Chemistry, College of Education for Pure Science Ibn-Al-Haitham, University of Baghdad, Baghdad, Iraq.
*Corresponding Author.

Received 03/01/2023, Revised 04/08/2023, Accepted 06/08/2023, Published Online First 20/03/2024

Abstract

4-((2-hydroxy-3,5-dinitrophenyl)diazenyl)-1,5-dimethyl-2-phenyl-1H-pyrazol-3(2H)-one was produced through the reaction of diazonium salt from 4-amino antipyrine with 2,4-dinitrophenol. This ligand is examined by (UV-Vis, FTIR,^{1}H,^{13}CNMR, and LC-Mass) spectral techniques and micro elemental analysis (C.H.N.O). Co(II), Ni(II), Cu(II), and Zn(II) complexes were also performed and depicted. Metal chelates were distinguished by utilizing flame atomic absorption, infrared analysis, and elemental, visible, as well as ultraviolet spectroscopy, in addition to conductivity and magnetic quantification. Methods of mole ratio and continuous contrast have been studied to determine the nature of the compounds. Beer's law was followed throughout a condensation reach of about 1×10^{-4} - 3×10^{-4} M/L. A higher molar absorbance was observed for compound solutions. Analytical data displayed all metal chelates in a 1:2 metal-ligand ratio. In general, the physicochemical data, and the octahedral geometry of the compounds are described. Compounds are tested in biological and dye studies

Keywords: azo dyes, biological activity, 4-aminoantipyrine, metal complexes, textile industry.

Introduction

Diverse types of dyes, often containing highly toxic metal complexes, have been used in the textile industry, and in other industries like the food industry, leather processing, papermaking, printing, paints, as well as cosmetics. These dyes constitute a source of grave concern to the environment through their discharge into fresh waters[1-3]. Because the azo group has several advantages, it is photochromic, oxidation- responsive, pH sensitive, and it can stabilize the oxidation state of low-valent metals due to the existence of a low-lying azo fastened π* molecular orbital, it has been utilized as a metal ion indicator for complex measurement of titration, and as dyes and pigments in textile industries [4,5]. These azo dye molecules make up over 70% of the entire amount of the dye used and have been reported to be mutagenic, 42 carcinogenic, and genotoxic to humans and other aquatic life forms [6]. Numerous uses of the dye's related electrolytes, from biology to the textile industry, have been discovered. If the dye is cytotoxic, it can be administered to the living cells after being wrapped in many electrolytes to boost its

Published Online First: March, 2024
https://doi.org/10.21123/bsj.2024.8319
P-ISSN: 2078-8665 - E-ISSN: 2411-7986
Baghdad Science Journal

biocompatibility. Additionally, pH detection is done using the dyes entrapped within the polyelectrolyte complexes[7]. The textile business has been revolutionized by polymer coloring reactions. In the production of food, essential electrolytes, and edible dyes are frequently used. Biological research has also discovered extensive usage for the combination of colors and proteins [8]. Recently, dyes are contained in nanosized polymers [9, 10].

Materials and Methods

Materials and reagent

The chemicals were applied as received from the provider: $CoCl_2.6H_2O$, $NiCl_2.6H_2O$, $CuCl_2.2H_2O$ also $ZnCl_2$ (Fluka), 2,4-dinitrophenol, 4-amino antipyrine (B.D.H).

Instrumentation

In the Agilent Technologies lab at the University of Tehran in Iran, ^{13}C and ^{1}H-NMR spectra were highlighted on a Brucker DRX type system (500MHz) in tetramethyl saline as a standard in dimethyl sulfoxide d6 solution. Using a Philips PW-Digital Conductance meter, the conductivity of the compounds dissolved in ethyl alcohol (10-3 M/L) was measured at 25 °C. Euro vector EA 3000, single V.3.O. was used to do micro elemental analysis (C.H.N.O.) Sherwood Applying the Auto Magnetic Susceptibility at 25 °C allowed scientists to refine the magnetic characteristics. A Shimadzu A.A-160A Atomic Absorption/Flame Emission Spectrophotometer was used to measure atomic absorbance. A UV-Vis-160A spectrophotometer was used to record the UV-visible spectrum. The spectral regions of the models were created as KBr disks and used to create the infrared spectrum of the Shimadzu, FTIR-8400S Fourier Transform Infrared Spectrophotometer at 4000-400 cm^{-1}. Shimadzu (E170 EV) Spectrometer measurements of mass spectrometry have been made. Otherwise, melting points were determined using the Stuart Melting Point Apparatus.

Preparation for the ligand

A Mixture of 10 mL ethanol and 2 mL HCl concentration was used to create a solution of 4-aminoantipyrine [11] (0.50 g, 1 mmole), which was then diazotized at 5 °C with a 10% $NaNO_2$ solution. A cool solution of ethyl alcohol containing 0.46 g and 1 mmole of 2,4-dinitrophenol was added to the denitrified solution for stirring. The precipitation of the azo ligand was then seen when 25 ml was observed in a dark-colored mixture containing 1 M NaOH solution. The precipitate was then filtered, recrystallized from hot ethanol and then allowed to dry. In Scheme 1, the interaction is depicted**.**

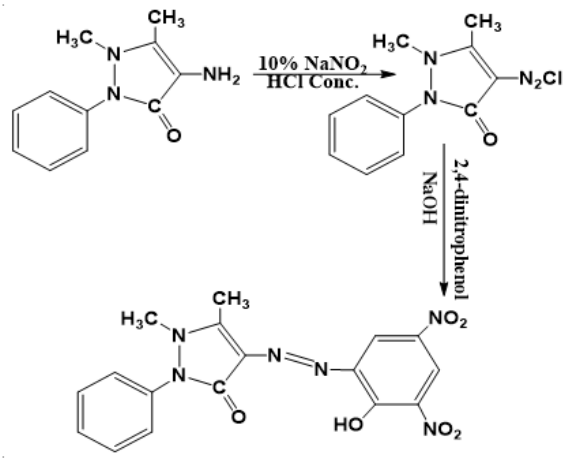

Scheme 1. Synthesis for azo-ligand (L).

Buffer solution

In one liter of doubly deionized water, ammonium acetate (0.01M, 0.771 gram) was dissolved. The pH range was maintained at (4–9) requiring the use of CH_3COOH or NH_3 solutions.

Standard solution

Mineral salt buffer solutions in a range between focus 10^{-5}-10^{-3} M/L were generated at pH 4-9. A significant volume of ethanolic ligand solutions with concentrations between 10^{-5}-10^{-3} M/L were created at the same time.

Metal chelate preparation

Ethyl alcohol solution from ligand (0.398gm, 2mmole) was added for stirring, using (0.118, 0.118, 0.085 and 0.064 gm, 1mmole) of metal chloride from (Co^{II}, Ni^{II}, Cu^{II} also Zn^{II}) and dissolved in the solution at the required pH. After filtering and washing with a 1:1 H_2O:C_2H_5OH solution, the liquid was chilled until the dark-colored precipitate was seen. Table 1 lists the physical parameters and analysis (CHNO), whereas Scheme 2 illustrates the preparation method.

Published Online First: March, 2024
https://doi.org/10.21123/bsj.2024.8319
P-ISSN: 2078-8665 - E-ISSN: 2411-7986
Baghdad Science Journal

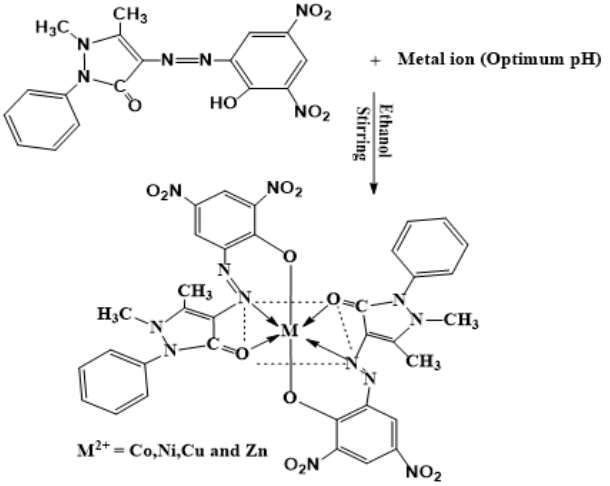

Scheme 2. Expected geometry for complexes with azo ligand.

Table 1. Physical characteristics for azo ligand as well their metal chelates.

Compounds	Color	M.P˚C	Yield %	Analysis Calc (Found) M%	C%	H%	N%	O%
Ligand(L)	Orange	130-132	88	-	51.25 (50.93)	3.51 (3.03)	21.10 (20.96)	24.12 (23.84)
$[Co(L)_2]$	Brown	120-122	83	6.91 (5.94)	47.83 (46.92)	3.04 (2.75)	19.69 (18.84)	22.50 (22.75)
$[Ni(L)_2]$	Reddish orange	156-158	85	6.80 (6.62)	47.88 (47.21)	3.05 (2.94)	19.71 (18.93)	22.53 (21.91)
$[Cu(L)_2]$	Deep brown	162-164	85	7.45 (6.97)	47.55 (46.91)	3.03 (2.96)	19.58 (18.87)	22.37 (21.81)
$[Zn(L)_2]$	Brown	146-148	82	7.56 (6.86)	47.49 (46.84)	3.02 (2.83)	19.55 (18.96)	22.35 (21.84)

Antimicrobial activity

The disc diffusion method was used to assess the ligand and all synthesized compounds for their in vitro antibacterial activities against (*Staphylococcus aureus, Staphylococcus epidermidis, and Psedomonas aeruginosa*) like Gram-positive bacteria as well as anti-fungal activities against *Candida albicans* (yeast) [12]. A model of 1-200 g/ml was employed along with the DMSO concentration and solvent used in the test samples. With any chemical, the fine diffusion technique is used to determine its antibacterial and antifungal activities. Sterilized Petri plates were filled with 1 cm^3 of a Gram-negative bacteria broth culture containing 106 CFU/cm3 of (*Streptococcus sp., Escherichia coli, and Klebsiella sp.*). Molten nutritious agar 15cm^3 has been preserved at temperature 45 ℃ as well as crowding at Petri-dishes as well as elastic to the stiffen. The other 6 mm holes were expertly filled with test solutions after being precisely bored with a sterile cork drill. For 24 hours, dishes were incubated around 37 °C.

Dyeing process

The chemicals are produced and applied via cotton fibers as (1% shade) offered dyeing qualities. The tissue dyeing continues for one hour at 15–20 ℃ and a pH of 10.

Results and Discussion

A combination of 4-aminoantipyrine and appropriate diazotized solutions from the base were effective for azo ligands (L). Microelemental analysis and spectrum analyses (^{13}C, $^{1}HNMR$, FT-IR, UV-Vis, and LC-Mass) were used to identify the generated azo ligand (C.H.N.O). To investigate the relationship between metal salts and the created ligand, aqueous-ethanol solutions were continuously obtained.

Published Online First: March, 2024
https://doi.org/10.21123/bsj.2024.8319
P-ISSN: 2078-8665 - E-ISSN: 2411-7986
Baghdad Science Journal

NMR spectra

Different signals may be seen in the ligand's ^{1}HNMR spectrum between δ=7.29 and 8.40 ppm, which are defined as aromatic protons[13]. At (δ=8.72) ppm, where the signals were detected, the value was determined to be (OH). Finding signals on (δ =3.16) ppm and (δ =2.10) ppm that, respectively, are characterized as (N-CH_3) and (CH_3) from pyrazole[14]. Water (D_2O) and DMSO-d_6 [15] signals at (δ =3.43 ppm) and (δ =2.50 ppm), respectively, are shown in Fig. 1 The pyrazole group's carbon in the ^{13}CNMR spectra from the ligand, exhibits resonance at (δ =19.01) as well as (δ =56.49) ppm. Carbon atoms from aromatic rings are responsible for the multiple signals at (=136.83, 129.76, 122.27, and 119.98) ppm. Signals owing to (C=O) and (C-OH) groups of carbon at (δ =157.89) ppm and (δ =138.71) ppm, respectively, as well as the indicative signal at (δ =39.40 ppm due to DMSO-d_6[16, 17], are shown in Fig. 2

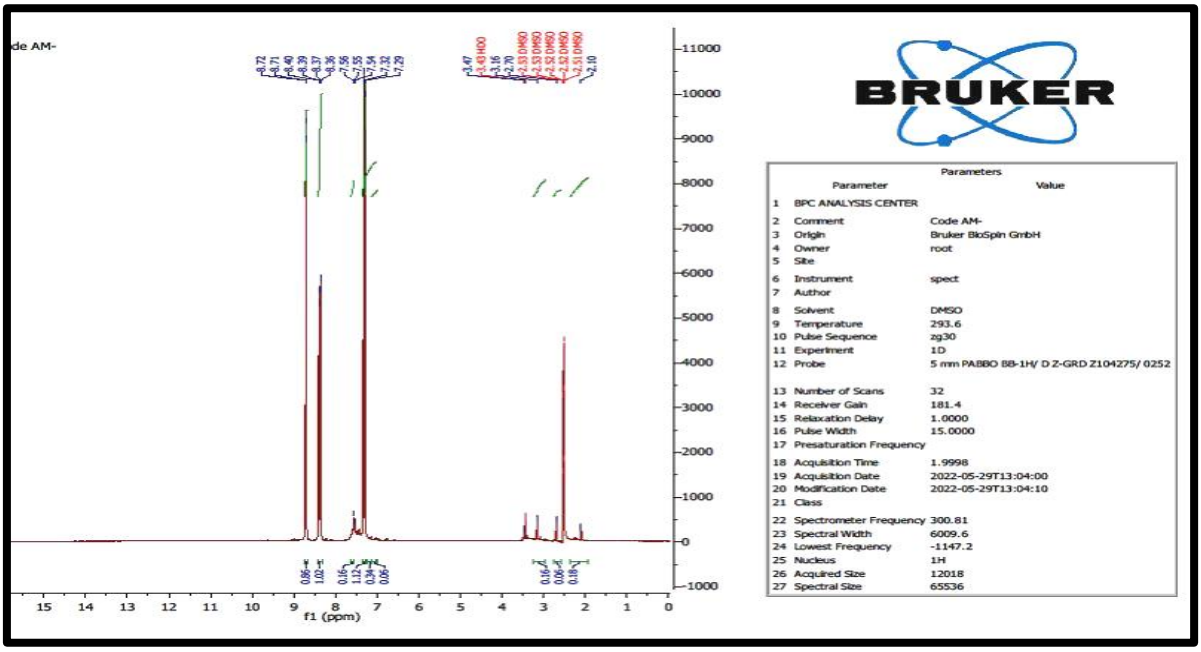

Figure 1. ^{1}HNMR spectrum for azo-ligand (L).

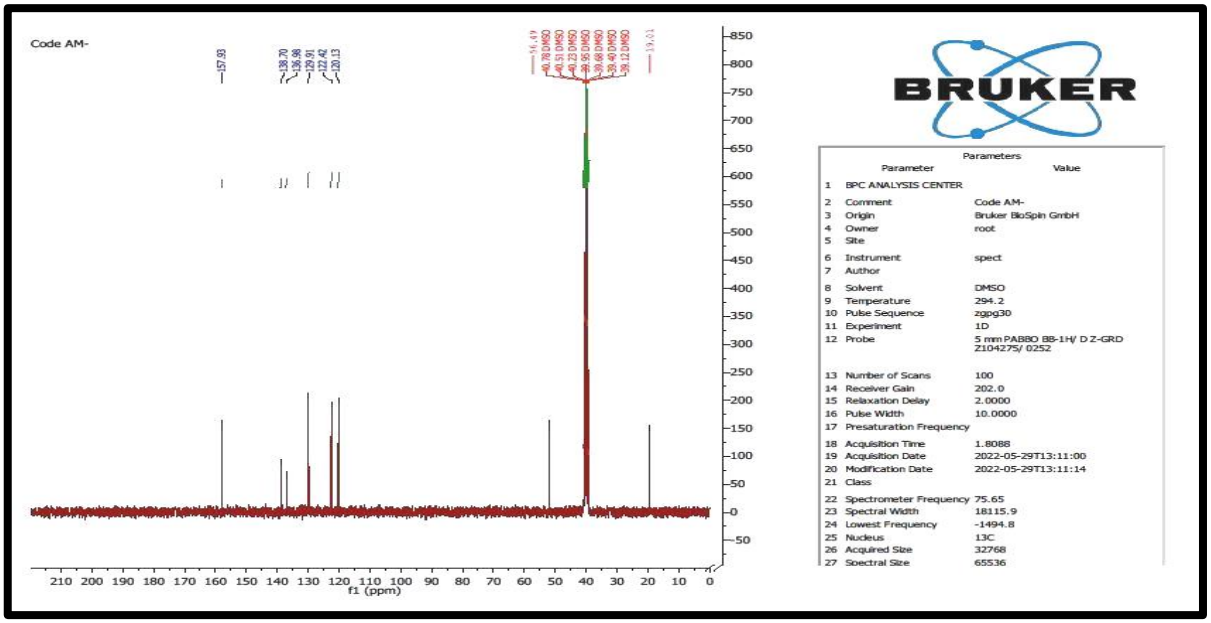

Figure 2. ^{13}CNMR spectrum for azo-ligand (L).

Published Online First: March, 2024
https://doi.org/10.21123/bsj.2024.8319
P-ISSN: 2078-8665 - E-ISSN: 2411-7986
Baghdad Science Journal

Mass spectrum

Due to the formula $C_{17}H_{14}N_6O_6$, the azo ligand mass spectrometry (L) revealed a peak centered at m/z = 398. Scheme 3 provides a summary of the segmentation's overall pattern. In Fig. 3 Because of the formulae $C_{34}H_{26}N_{12}O_{12}Ni$ and $C_{34}H_{26}N_{12}O_{12}Cu$, the complexes' mass spectra show peaks centered at m/z = 852 and 858, respectively. Schemes 4 and 5 provide an overview of the segmentation pattern in general. Figs. 4 and 5 are shown.

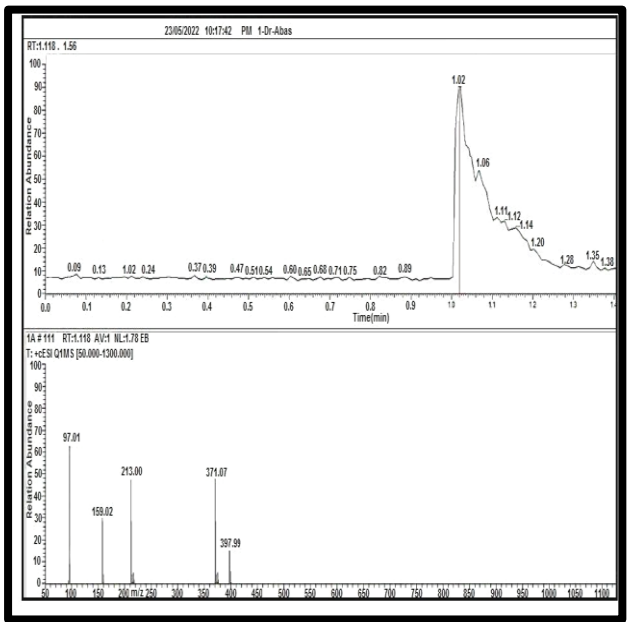

Figure 3. Mass spectrum for azo-ligand (L).

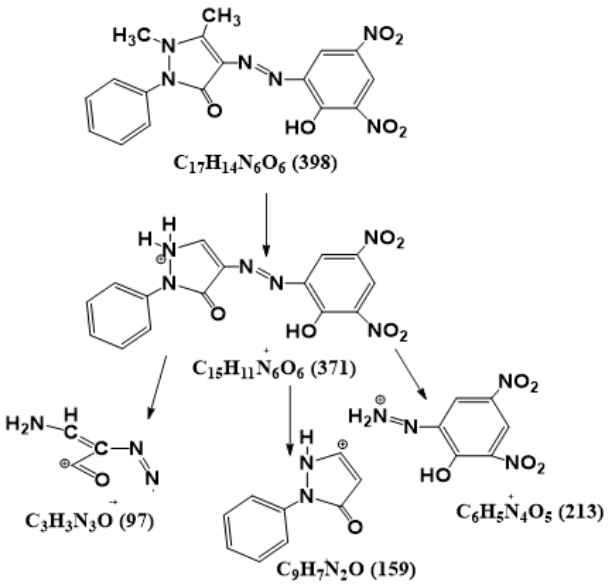

Scheme 3. Retail style for azo-ligand (L).

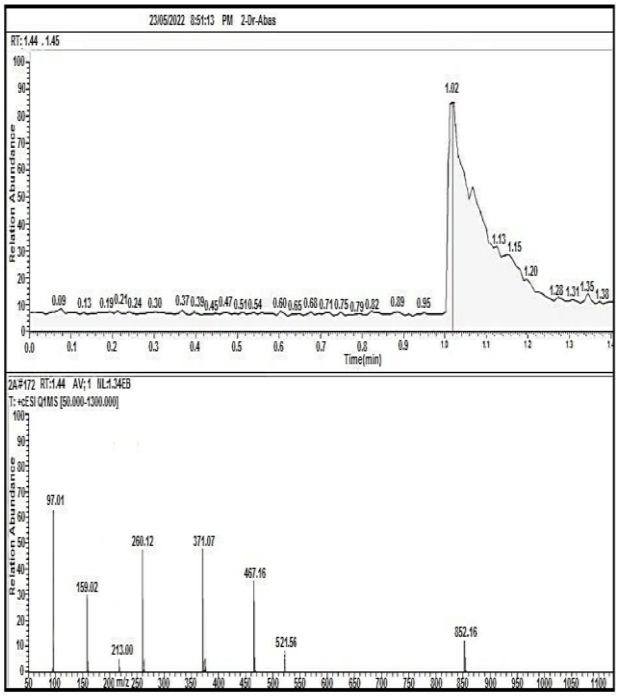

Figure 4. Mass spectrum as $[Ni(L)_2]$ complex.

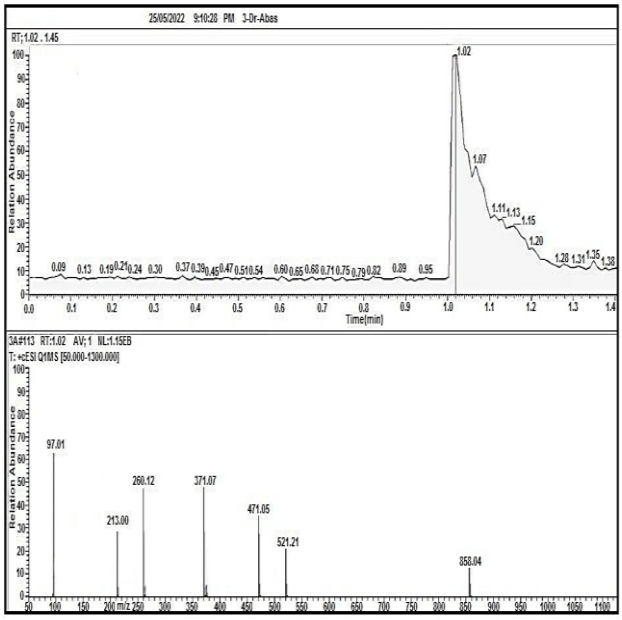

Figure 5. Mass spectrum as $[Cu(L)_2]$ complex.

Published Online First: March, 2024
https://doi.org/10.21123/bsj.2024.8319
P-ISSN: 2078-8665 - E-ISSN: 2411-7986
Baghdad Science Journal

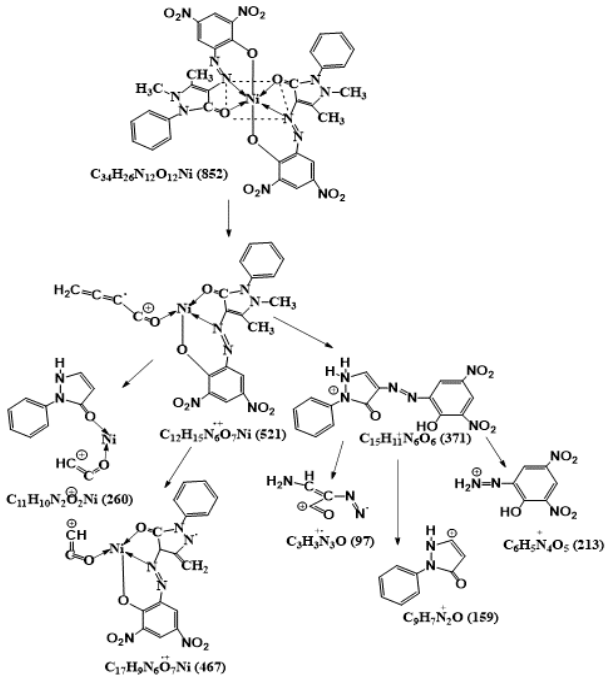

Scheme 4. Retail style for $[Ni(L)_2]$ complex.

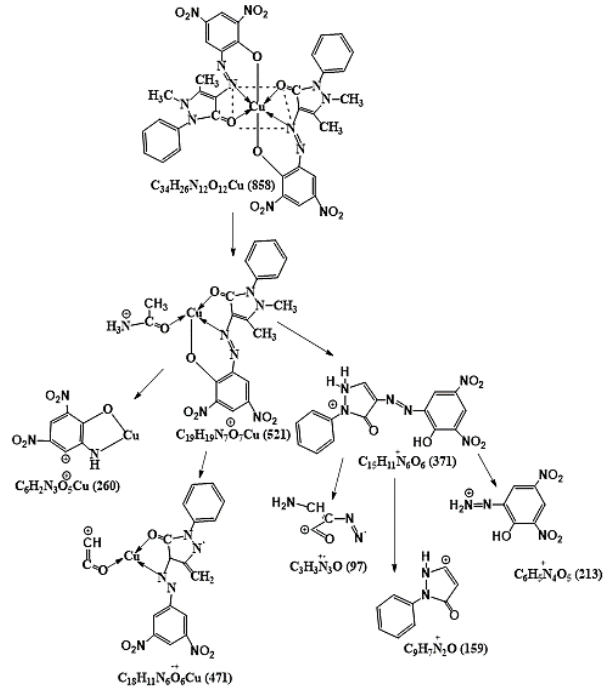

Scheme 5. Retail style for $[Cu(L)_2]$ complex.

Calibration curve

Only (1-3 x 10^{-4} M/L) of the various molar concentrations 10^{-5}-10^{-3} M/L with combined aqueous ethyl alcohol ligand as well as metal ions matched Beer's law and displayed a distinct bright hue. For the correlation factor R > 0.998 as seen in Fig. 6, choosing the best and most suitable straight lines.

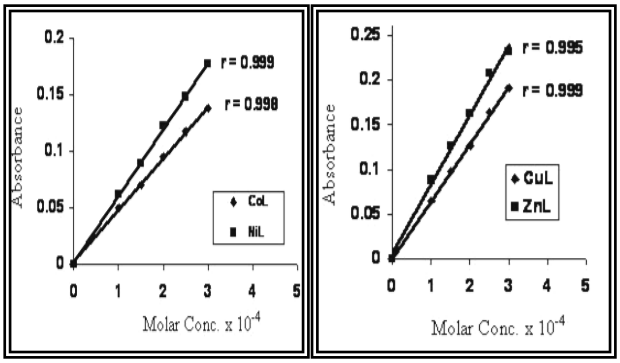

Figure 6. Linear relationship between molar concentration and absorbance obtained for the $[ML_2]$.

Model conditions

The first test to look for interactions between generated ligand and the under-taught metal ions when manufacturing compounds is the spectrum of mixing solutions of ligand and metal ions to get a better pH as well as focus, and a consistent wavelength (max). The ratio of metal to ligand (M:L) was also defined in the generated molecules. The solution that gave the maximum absorption at a constant (max) with varying pH was chosen as the optimal concentration, and the findings are shown in Table 3. The experiment's findings demonstrate all synthesized compounds' absorbance in a buffer solution of NH_4OOCCH_3 at pH 4-9. As realized in Fig.7, every chemical that has been created has the correct PH.

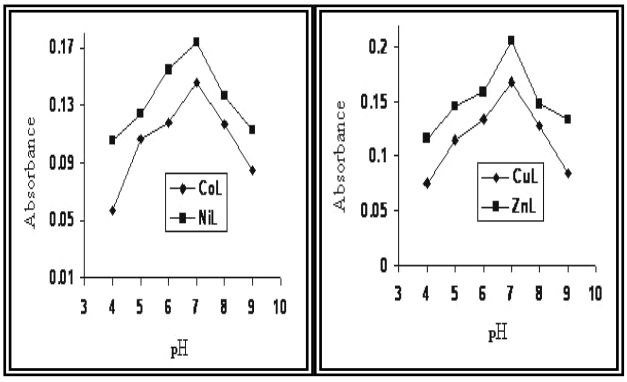

Figure 7. Effect of pH variation on the absorbance (λ_{max}) of the $[ML_2]$ complexes.

Metal into ligand ratio

By using mole ratio and function, the assignment to complexes in solutions was validated. The outcomes are dispersed in a 1:2 ratios in both situations (metal

Published Online First: March, 2024
https://doi.org/10.21123/bsj.2024.8319
P-ISSN: 2078-8665 - E-ISSN: 2411-7986
Baghdad Science Journal

to ligand). The chosen piece of land is presented in Fig. 8.

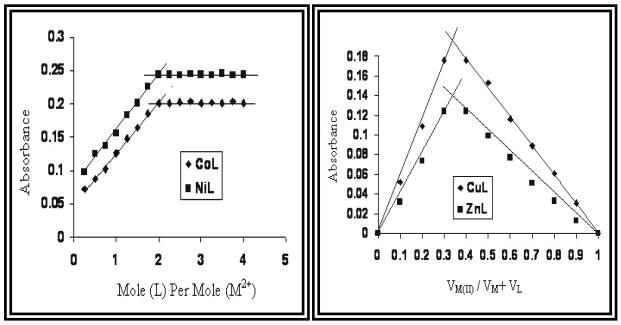

Figure 8. Mole ratio and Job's method evaluation of the [ML_2] complexes.

The Effect of time

This reaction was completed within 5 minutes. The temperature was fixed at 25 °C, then was maintained stable for about 90 minutes, and this is due to the strong coordination of bonds with metal-salts. The results are displayed in Fig. 9.

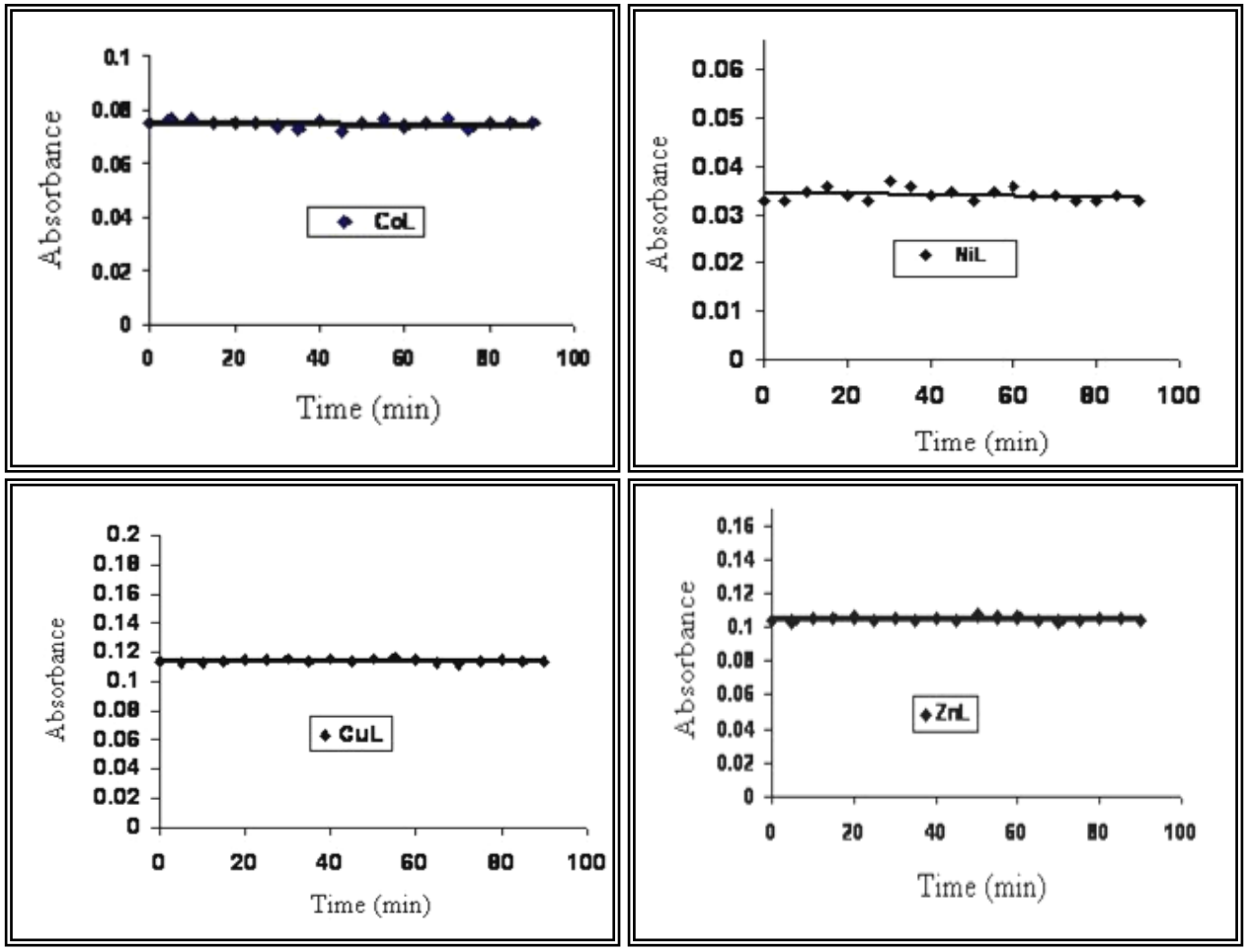

Figure 9. Effect of time for the stability of the [ML_2] complexes.

Stability Constant as well as Gibbs free energy

The stability constant (K) into (1:2) metal to ligand compound can be subtracted depending on Eqs. 1and 2.

$$K = \frac{1-\alpha}{4\alpha^3 C^2} \quad .....1 \quad , \quad \alpha = (Am - As)/Am.....2$$

Where C denotes the concentration point for complex solutions at mol/L, As denotes the

Published Online First: March, 2024
https://doi.org/10.21123/bsj.2024.8319
P-ISSN: 2078-8665 - E-ISSN: 2411-7986
Baghdad Science Journal

absorbance of a solution containing the same amount of ligand as well as metal ions, α denotes the degree of dissociation, and Am denotes the adsorption of a solution containing the same amount of metal as well as excess ligand. High values of (K) denote highly stable manufactured chemicals[18]. Investigations were made on the Gibbs free energy's (G) thermodynamic properties. G values [19] were determined using Eq. 3.

$$\Delta G = -R\ T\ Ln\ k \quad \ldots\ldots\ldots\ldots 3$$

Where R is a gas constant which is equal to 8.314 $J.mol^{-1}.K$, T is absolute temperature in Kelvin. The negative value of (ΔG) which could be seen in Table 2 is due to the spontaneous reaction between the azo dye ligand (L) and metal ions [20].

Table 2. Stability constant and Gibbs free energy of the produced compounds.

Complexes	A_s	A_m	α	k	Lin k	ΔG $kJ.mol^{-1}$
$[Co(L)_2]$	0.126	0.201	0.373	78.375×10^6	18.177	- 45.034
$[Ni(L)_2]$	0.156	0.244	0.360	$.181\times10^658$	17.880	- 44.298
$[Cu(L)_2]$	0.093	0.176	0.471	21.160×10^6	16.867	- 41.789
$[Zn(L)_2]$	0.052	0.124	0.580	13.548×10^6	16.421	- 40.684

Physical characteristics

Ratio of chelation was (1:2) (Metal:Ligand) was produtced through interaction from ligand-melted at ethyl alcohol for metal ions melted at perfect pH. Outcome from element analysis as well as the import for the metals from the compounds had accurate, actual same values. The conductivities of metal chelates which were melted at ethanol (10^{-3} M/L) non-electrolytic[21] exposure are shown in Table 3.

Electronic spectral

The UV spectrum of produced compounds melted with ethyl alcohol (10^{-3} M/L) was measured and the data are included in Table 3. The UV spectrum of the azo ligand exhibits peaks on 223, 288 and 394 nm specified for the moderate energy (π-π*) transition [22]. $Co^{(II)}$ spectrum appeared to have three peaks on 225, 311, and 448 nm due to intra ligand and charge transfer. Peaks on 566, 680, and 724 nm are assigned to the electronic transition type $^4T_{1g(F)} \rightarrow {}^4T_{1g(P)}$, $^4T_{1g(F)} \rightarrow {}^4A_{2g}$ and $^4T_{1g(F)} \rightarrow {}^4T_{2g(F)}$ successively, the magnetic moment for the complex was recorded at 4.82 B.M that was very close to the octahedral environment [23]. The spectrum of the $Ni^{(II)}$ complex exhibits peaks at 228, 310, and 438 nm that were components of the ligand field and charge transfer. Another peak at 546, 663, and 710 nm points out the electronic transition type $^3A_{2g} \rightarrow {}^3T_{1g(P)}$, $^3A_{2g} \rightarrow {}^3T_{1g(F)}$, and $^3A_{2g} \rightarrow {}^3T_{2g(F)}$. The value for the magnetic moment on 2.93 B.M was included as an extra affirmation for the octahedral geometry [24]. The electronic spectrum for the $Cu^{(II)}$ showed peaks at 233, 344, and 485 nm because of the intra ligand and charge transfer, also peaks at 680 nm qualified for the electronic transition type $^2E_g \rightarrow {}^2T_{2g}$. In addition, the magnetic moment for the complex has been recorded at 1.74 B.M which is so close to the octahedral environment [25]. $Zn^{(II)}$ complex gave an indication for the charge transfer, also magnetic susceptibility showed that complexes had diamagnetic moments. It could be indicated that the outcome for the (d-d) transition is not expected hence electronic spectrum did not confer with the productive data, from this point of view, it seems that the outcome is a good idea of the previous work from octahedral [26].

Published Online First: March, 2024
https://doi.org/10.21123/bsj.2024.8319
P-ISSN: 2078-8665 - E-ISSN: 2411-7986
Baghdad Science Journal

Table 3. Conditions for the compounds produced as well as UV- Visible, magnetic susceptibility also conductivity mensurations data.

Compounds	Optimum pH	Optimum Molar Conc. x 10-4	M:L Ratio	(λmax) nm	ABS	Єmax (L.mol-1.cm-1)	Λm(S.cm2.mol-1) In ethanol	μeff (B.M)
Ligand(L)	-	-	-	218 290 410	2.198 0.785 2.340	2198 0.785 2.340	-	-
[Co(L)2]	7	2.0	1:2	225 311 448 566 680 724	2.154 0.975 0.431 0.044 0.032 0.025	2154 975 431 44 32 25	11.67	4.82
[Ni(L)2]	7	2.5	1:2	228 310 438 546 663 710	2.187 0..974 0.455 0.083 0.073 0.036	2187 974 455 83 73 36	15.45	2.93
[Cu(L)2]	7	2.5	1:2	233 344 485 680	2.017 0.765 0.448 0.088	2017 765 448 88	12.63	1.74
[Zn(L)2]	7	2.0	1:2	232 352 482	2.264 0.843 0.296	2264 843 296	10.52	Dia

FTIR spectra

Azo ligand and metal chelate data were combined, and they are shown in Table 4. Ligand spectral analysis for the (OH) phenol showed bands at the 3267 cm^{-1} stretching vibration. The disappearance of the band on the spectra of the compounds created indicates that the phenol group had been de-protonated into a coordination for the metal ion [27]. The band at 1624 cm^{-1} was deleted for the lower frequency inclusion of the coordination for the metal ion because of the (C=O) group [28]. The vibration from (C=C) was qualified for the band at 1535 cm^{-1}. Band at 1477 cm^{-1} was deleted for the higher frequency inclusion of the coordination for the metal ion because of the (N=N) group [29], extending the frequency bands for metal-nitrogen at a different rate than metal-oxygen [30, 31].

Table 4. The main frequencies for azo ligand and metal chelates (cm^{-1}).

Compounds	υ (OH)	υ (C=O)	υ (C=C) + υ (N=N)	υ(M-N) + υ (M-O)
Ligand(L)	3267 br.	1624 sh.	1535 s. 1477 sh.	-
[Co(L)2]	-	1600 sh..	1535 s. 1481 sho.	578 w. 520 w.
[Ni(L)2]	-	1600 sh.	1531 s. 1481 sh.	520 w. 428 w.
[Cu(L)2]	-	1600 sh.	1531 s. 1481 sh.	574 w. 520 w.
[Zn(L)2]	-	1604 sh.	1531 sh. 1481 sh.	578 w. 447 w.

Where Shrefers to sharp, Srefers to strong, Shorefers to shoulder andWrefers to weak.

Published Online First: March, 2024
https://doi.org/10.21123/bsj.2024.8319
P-ISSN: 2078-8665 - E-ISSN: 2411-7986
Baghdad Science Journal

Antimicrobial testing outcome

Using the disc diffusion technique, azo ligand (L) complexes were also assessed for their anti-bacterial efficiency against, Gram-positive bacteria (*Staphylococcus epidermidis, Staphylococcus aureus, and Psedomonas aeruginosa*), anti-fungal activities against *Candida albicans*, and Gram-negative bacteria (*Escherichia coli, Streptococcus sp., and Klebsiella sp.*). The inhibition area of the ligand and their complexes was evaluated in millimeters for the antibacterial and antifungal activities, the data is presented in Table 5. These complexes all exhibited antibacterial and antifungal properties.

Table 5. Biological efficiency outcomes for azo ligand (L) as well as complexes exhibited the suppression diameter in (ml) of the bacteria within 24 hour.

Compounds	*Staphyl-ococcus aureus (G+ev)*	*Staphyloco-ccus epidermidis (G+ev)*	*Psedomonas Aeruginaso (G+ev)*	*Steptococcus sp. (G-ev)*	*Escherichia coli (G-ev)*	*Klebsiella sp. (G-ev)*	*Candida albicans (Yeast)*
Control (DMSO)	-	-	-	-	-	-	-
Ligand(L)	8	15	14	12	11	10	10
$[Co(L)_2]$	10	12	13	14	10	13	12
$[Ni(L)_2]$	13	10	8	10	12	11	9
$[Cu(L)_2]$	9	11	10	9	13	12	12
$[Zn(L)_2]$	16	14	15	14	14	15	16

Performance of dyeing

It has already been determined how well the completed chemicals dye cotton fabrics. The colors functioned as a component of the detergent's brightness and stability. Therefore, complete dyes exhibit superb dyeing stability and textural depth. Coloring is seen in Fig. 10.

Ligand

$[Co(L)_2]$

$[Ni(L)_2]$

$[Cu(L_2)_2]$

$[Zn(L)_2]$

Figure 10. Textiles dyeing for azo ligand and metal chelates.

Published Online First: March, 2024
https://doi.org/10.21123/bsj.2024.8319
P-ISSN: 2078-8665 - E-ISSN: 2411-7986
Baghdad Science Journal

Conclusion

In this study, an azo ligand has been used to produce metal ion complexes. The melting point, spectroscopic analyses, conductivity, and magnetic quantifications were used to describe the substances. Antimicrobial activity exploration was carried out in against tested organism. The data from the results imply that the produced compounds have an octahedral

Acknowledgment

We would like to acknowledge the Department of Chemistry and College of Education for Pure Science /Ibn-Al-Haitham, University of Baghdad.

Authors' Declaration

- Conflicts of Interest: None.
- We hereby confirm that all the Figures and Tables in the manuscript are ours. Furthermore, any Figures and images, that are not ours, have been included with the necessary permission for re-publication, which is attached to the manuscript.
- Authors sign on ethical consideration's approval.
- Ethical Clearance: The project was approved by the local ethical committee in University of Baghdad.

Authors' Contribution Statement

The work was carried out in collaboration all authors. A. O. H. and R. A. A. synthesis and characterization of the ligand. J. M. M., wrote and edited the manuscript with revisions idea. A. J. J., synthesis and characterization of the metal complexes. All authors read and approved the final manuscript.

References

1. Fleischmann C, Lievenbrück M, Ritter H. Polymers and dyes: Developments and applications. Polymers. 2015; 7: 717–746. https://doi.org/10.3390/polym7040717.
2. Zhang H, Chan-Park M B, Wang M. Functional polymers and polymer–dye composites for food sensing, Macromol. Rapid Commun. 2020; 41: 1–17.https://doi.org/10.1002/marc.202000279.
3. Myek B, Sunday N, Agbamu O F. Synthesis and characterization of an azo dye and its iron complex.Fudma. J Sci. 2021; 5(4): 347-352. doi: https://doi.org/10.33003/fjs-2021-0504-750.
4. Alabidi1 H M, Farhan A M, Salh N S, Aljanaby A A J. New azo-Schiff compounds and metal complexes derived from 2-naphthol synthesis, characterization, spectrophotometric, and study of biological activity. Current Appl Sci Techn. 2023; 23(4): 1-14. https://doi.org/10.55003/cast.2022.04.23.007.
5. Moamen S R, Altalhi T, Safyah B B, Ghaferah H A, Kehkashan A. New Cr(III), Mn(II), Fe(III), Co(II), Ni(II), Zn(II), Cd(II),and Hg(II) Gibberellate Complexes: Synthesis, structure, and inhibitory activity against COVID-19 protease. Russ J Gen Chem. 2021; 91(5): 890–896. https://doi.org/10.1134/S1070363221050194.
6. Maurice K, Mariam AC, Katia NN, Awawou GP, Sally-Judith EN, Peter TN. Synthesis, characterization and antimicrobial studies of Co(II), Ni(II), Cu(II) and Zn(II) complexes of (E)-2-(4-dimethylbenzydimino)-glycylglycine,(Glygly-DAB) a Schiff base derived from 4-dimethylaminobenzaldehyde and glycylglycine. Int J Org Chem. 2018; 8: 298-308. https://doi.org/10.4236/ijoc.2022.124015.
7. Hamza IS, Mahmmoud WA, Al-Hamdani AAS, Ahmed SD, Allaf AW, AlZoubi W. Synthesis, characterization, and bioactivity of several metal complexes of (4-Amino-N-(5-methyl-isaxazol-3-yl)-benzenesulfonamide). Inorg Chem Commun. 2022; 24(144): 109776. https://doi.org/10.1016/j.inoche.2022.109776.
8. Dahi MA, Jarad A J. Synthesis, characterization and biological evaluation of thiazolyl azo ligand complexes with some metal ions. J Phys Conf. 2020; 1664(012090): 1-18. https://doi.org/10.1088/1742-6596/1664/1/012090.
9. Jana B, Bhattacharyya S, Patra A. Perspective of dye-encapsulated conjugated polymer nanoparticles for potential applications, Bull Mater Sci. 2018; 41: 122. https://doi.org/10.1007/s12034-018-1643-x.

Published Online First: March, 2024
https://doi.org/10.21123/bsj.2024.8319
P-ISSN: 2078-8665 - E-ISSN: 2411-7986
Baghdad Science Journal

10. Oyarce E, Butter B, Santander P, Sánchez J. Polyelectrolytes applied to remove methylene blue and methyl orange dyes from water via polymer-enhanced ultrafiltration. J Environ Chem Eng. 2021; 9(6): 106297. https://doi.org/10.1016/j.jece.2021.106297.
11. Nair MLH, Mathew G, Kumar MRS. Synthesis and characterization of some new Cu(II) complexes of azo dyes derived from 1,2-dihydro-1,5-dimethyl-2-phenyl-4-amino-3H-pyrazol-3-one. Indian J Chem. 2005; 44: 85-89.
12. Li J, Fan J, Cao R, Zhang Z, Du J, Peng X. Encapsulated dye/polymer nanoparticles prepared via miniemulsion polymerization for inkjet printing. ACS Omega. 2018; 3: 7380–7387. https://doi.org/10.1021/acsomega.8b01151.
13. Hussein AO, Abbas RA, Sultan JS, Jarad AJ. Synthesis and characterization of metal(II) complexes with azo dye ligand and their industrial and biological applications. Egypt J Chem. 2021; 64(11): 6717-6724. https://doi.org/10.21608/EJCHEM.2021.68770.3530.
14. Kirill VY, Aleksandr SS, Werner K, Sergey AG. Synthesis, crystal chemistry of octahedral Rhodium(III) Chloroamines. Molecules. 2020; 25(768): 1-17. https://doi.org/10.3390/molecules25040768.
15. Al-Khazraji AMA, Al Hassani RAM. Synthesis, characterization and spectroscopic study of new metal complexes form heterocyclic compounds for photostability study. Syst Rev Pharm. 2020; 11(5): 535-555.
16. Al-Sheikh M, Medrasi HY, Sadek KU, Mekheimer RA. Synthesis and spectroscopic properties of new azo dyes derived from 3-ethylthio-5-cyanomethyl-4-phenyl-1,2,4-triazole. Molecules. 2014; 19(3): 2993-3003. https://doi.org/10.3390/molecules19032993.
17. Shaalan N D, Abdulwahhab S. Synthesis, characterization and biological activity study of some new metal complexes with Schiff's bases derived from [o-vanillin] with [2-amino-5-(2-hydroxy-phenyl)-1,3,4-thiadiazole]. Egypt J Chem. 2021; 64(8): 4059-4067. https://doi.org/10.21608/EJCHEM.2021.66235.3432.
18. Kirill VY, Aleksandr SS, Werner K, Sergey AG. Synthesis, Crystal Chemistry of Octahedral Rhodium(III) Chloroamines. Molecules. 2020; 25(768): 1-17. https://doi.org/10.3390/molecules25040768.
19. KofiKyei S, Onyewuchi A, Godfred D. Synthesis, characterization and antimicrobial activity of peanut skin extract-azo-compounds. Sci Afr. 2020; 8 (e00406): 1-14.https://doi.org/10.1016/j.sciaf.2020.e00406.
20. Al-Daffy RKH, Al-Hamdani AAS. Synthesis, characterization, and thermal analysis of a new acidic azo ligand's metal complexes. Baghdad Sci J. 2022; 3(19): 121-133. https://doi.org/10.21123/bsj.2022.6709.
21. GearyWJ. The use of conductivity measurements in organic solvents for the characterisation of coordination compounds. Coord Chem Rev. 1971; 7: 81-122. http://dx.doi.org/10.1016/S0010-8545(00)80009-0.
22. Saadi L, Ghali AA. Synthesis and characterization of some metal complexes derived from azo ligand of 4,4' methylenedianiline and resorcinol. Biomed Chem Sci. 2022; 1(4): 241-248. https://doi.org/10.48112/bcs.v1i4.252.
23. Raghavendra KR, Kumar KA. Synthesis of some novel azo dyes and their dyeing, redox and antifungal properties, Int J Chem Tech Res. 2013; 5(4): 1756-1760.
24. Ravanasiddappa M, Sureshg T, Syed K, Radhavendray SC, Basavaraja C, Angadi SD. Transition metal complexes of 1,4(2-hydroxyphenyl-1-yl)di-iminoazine:synthesis, characterization and antimicrobial studies, E-J Chem. 2008; 5(2): 395-403. https://doi.org/10.1155/2008/328961.
25. Al-Khateeb Z T, Karam F F, Al-Adilee K. Synthesis and characterization of some metals complexes with new heterocyclic azo dye ligand 2-[2-(5- Nitro thiazolyl) azo]-4- methyl -5- nitro phenol and their biological activities. J Phys Conf. 2019; 1294 (052043): 1-18. https://doi.org/10.1088/1742-6596/1294/5/052043.
26. Kilinc D, Şahin O, Horoz S. Use of low-cost Zn(II) complex efciently in a dye-sensitized solar cell device. J Mater Sci Mater Electron. 2019; 30: 11464–11467. https://doi.org/10.1007/s10854-019-01497-5.
27. Oloyede H O, Woods J A O, Gorls H, Plass W, Eseola A O. N-donor-stabilized Pd(II) species supported by sulphonamide-azo ligands: Ligand architecture, solvent co-ligands, CeC coupling. J Mol Struct. 2020; 1199(127030): 1-11. https://doi.org/10.1016/j.molstruc.2019.127030.
28. Anacona J, Pineda Y, Bravo A, Camus J. Synthesis, characterization and antibacterial activity of a tridentate Schiff base derived from Cephalexin and 1,6-hexanediamine and its transition metal complexes. Med Chem. 2016; 6(7): 467-473. https://dx.doi.org/10.4172/2161-0444.1000385.
29. Sahap EH, Sajad FAA, Al-Labban HMY. Incorporation of nickel with azo dye and its applications in dye-sensitized solar cells. Int J Drug Del Tech. 2022; 12(2): 603-609.
30. Lateef SM , Ismail AA . Synthesis a novel complexes of VO(II),Mn(II),Fe(II) ,Co(II), Ni(II), Cu(II)and Pt(IV) derived from Schiff's base of pyridoxal and 2-amino-4-nitrophenol and study their biological activates. Ibn Al-Haith J Pur Appl Sci. 2023; 36(2): 259-275. https://doi.org/10.30526/36.2.3054.
31. Abdulammer JH, Alis MF. Heavy metal complexes of 1,2,3-triazole derivatives: synthesis, characterization, and cytotoxicity appraisal against breast cancer cell lines (MDA- MB-231). Baghdad Sci J. 2022; 19(6): 1410-1422.https://doi.org/10.21123/bsj.2022.7178.

Published Online First: March, 2024
https://doi.org/10.21123/bsj.2024.8319
P-ISSN: 2078-8665 - E-ISSN: 2411-7986
Baghdad Science Journal

تحضير وتشخيص ودراسة صناعية وبايولوجية لليكاند صبغة الآزو وبعض أيوناتة الفلزية

عباس عبيد حسين [1]، رنا عبدالإله عباس [2]، جنان محمد محمود الزنكي [3]، عامر جبار جراد[4]

[1]قسم المختبرت التكنلوجية الطبية، كلية التكنلوجية الطبية ، الجامعة الإسلامية- النجف ، العراق.
[2]قسم الصناعات الكيمياوية ، المعهد التقني ، الجامعة التقنية الوسطى، بغداد،العراق.
[3]قسم الكيمياء، كلية العلوم ، جامعة ديالى، ديالى،العراق.
[4]قسم الكيمياء ، كلية التربية للعلوم الصرفة ابن الهيثم ، جامعة بغداد، بغداد،العراق.

الخلاصة

حضر 4-((2-هيدروكسي-5،3- ثنائي نيترو) دايازنيل) 5،1-ثنائي مثيل- 2-فنيل-1بايرازول-3-((H2-اون من مفاعلة ملح الدايازونيوم للمركب 4-امينو انتي بايرين مع 4،2- ثنائي نيتروفينول. تم تشخيص الليكاند بوساطة طيف الأشعة فوق البنفسجية- المرئية والأشعة تحت الحمراء وطيف الرنين النووي المغناطيسي للبروتون والكاربون وطيف الكتلة ، فضلا عن قياس التحليل الدقيق للعناصر(C.H.N.O) . حضرت معقدات الكوبلت (II) والنيكل (II)والنحاس(II) والخارصين(II) وشخصت بوساطة تقنية الامتصاص الذري اللهبي واطياف الأشعة فوق البنفسجية- المرئية والأشعة تحت الحمراء والتحليل الدقيق للعناصر(C.H.N.O)، فضلا عن قياسات التوصيلية المولارية والحساسية المغناطيسية. درست تراكيب المعقدات باستخدام طريقتي النسب المولية والمتغيرات المستمرة، وخضعت محاليل هذه المعقدات لقانون لامبرت – بير ضمن مدى التراكيز - 3×10-4 1×10 (M)، اشارة النتائج التحليلية ان نسبة فلز: ليكاند هي (1:2). ومن خلال النتائج التحليلية تم اقتراح الشكل ثماني السطوح للمركبات المحضرة ، كما تم اختبار المركبات المحضرة للدراسات الصناعية والبايولوجية.

الكلمات المفتاحية: اصباغ الآزو ، الفعالية البايولوجية ،4-امينوانتيبيرين، معقدات العناصر، الخيوط الصناعية.